Electronic Supplementary Material (ESI) for RSC Advances.

One-step synthesis of nanohybrid CDs-TiO_2 composites with enhanced ultraviolet light active photocatalysis

Fan Li, Feng Tian,* Changjun Liu, Zheng Wang, Zhenjie Du, Ruixin Li, Li Zhang

Institute of Medical Equipment, Academy of Military Medical Sciences, Tianjin 300161, PR China

TABLE S1: Crystalline characterization of different samples

Sample	2θ	d[a] (nm)	FWHM	CS[b] (nm)
C-6	25.280	0.352	1.011	8.1
C-9	25.500	0.349	0.848	9.7
C-12	25.102	0.354	0.690	11.9

[a] Determined by XRD using the Bragg equation. [b] Determined by XRD using the Scherrer equation.

The interplanar crystal spacing (d) and average crystallite sizes (CS) of the as-prepared C/TiO_2 samples are shown in Table 1, which were estimated using the Bragg equation (Ⅰ) and Scherrer equation (Ⅱ) as follows, respectively.

$$d = \frac{n \cdot \lambda}{2\sin\theta} \quad \text{Ⅰ}$$

$$CS = \frac{k \cdot \lambda}{FWHM \cdot \cos\theta} \quad \text{Ⅱ}$$

Where FWHM is the half-height width of the diffraction peak of anatase or rutile, k = 0.89 is a coefficient, θ is the diffraction angle, and λ is the X-ray wavelength corresponding to the Cu Kα radiation.

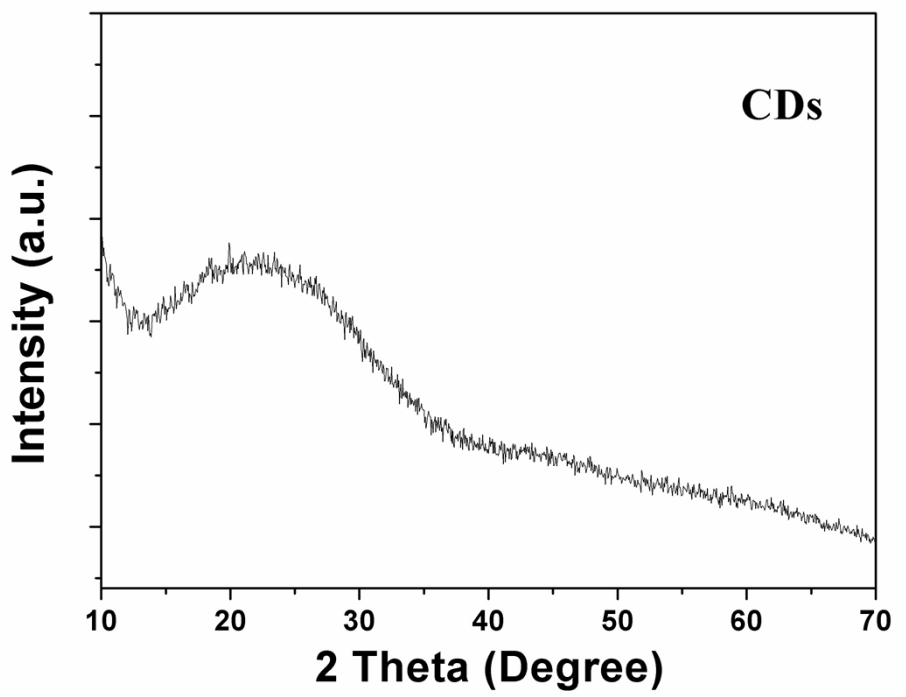

Fig. S1 XRD pattern of the as-prepared pure CDs.

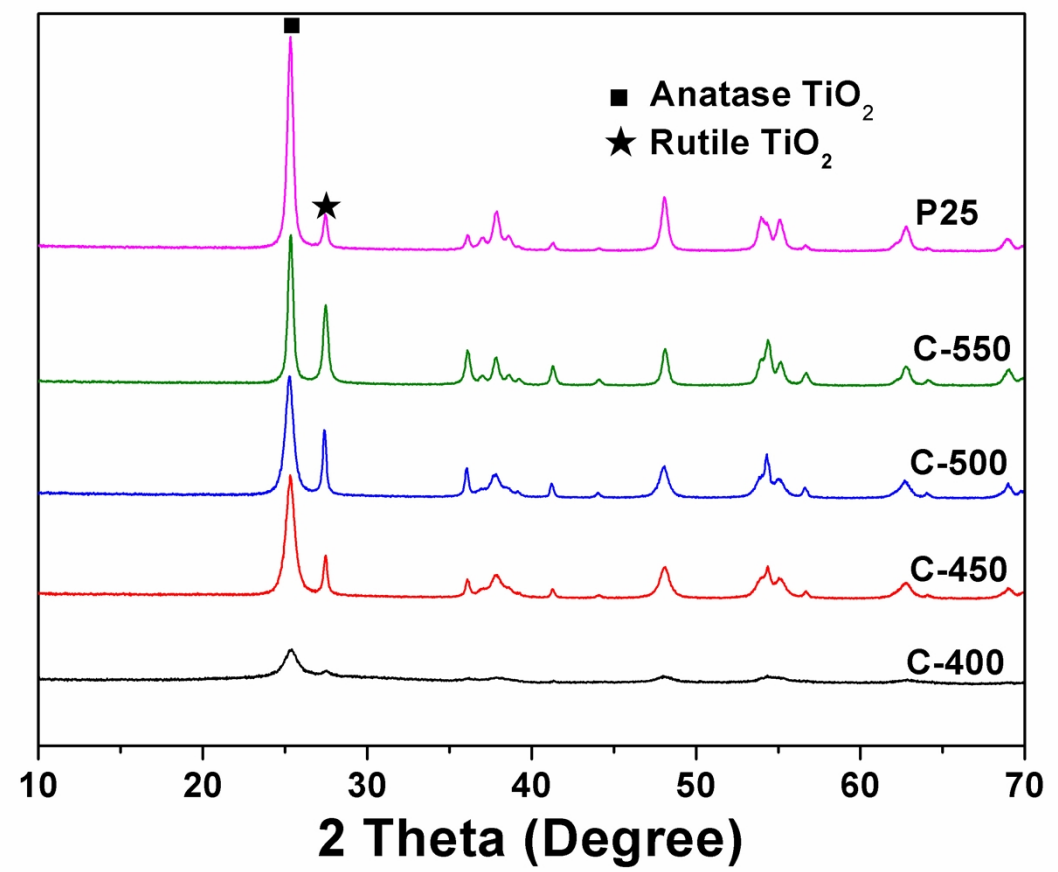

Fig. S2 XRD patterns of the commercial Degussa P25 and further annealed composites under different temperatures.

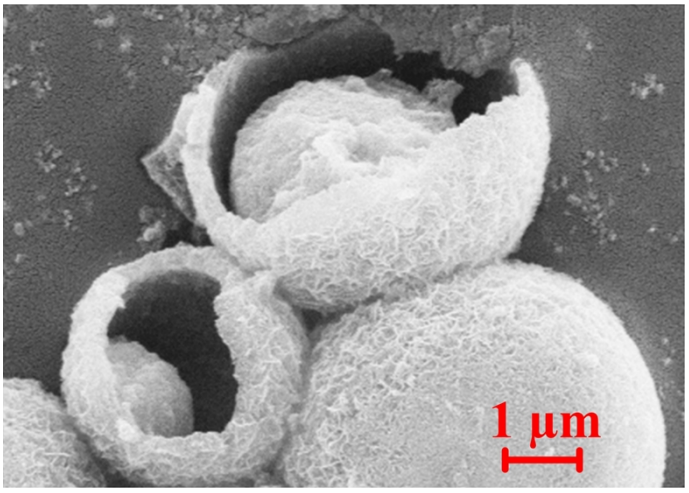

Fig. S3 SEM image of partial broken microspheres in sample C-12 (scale bar: 1 μm).

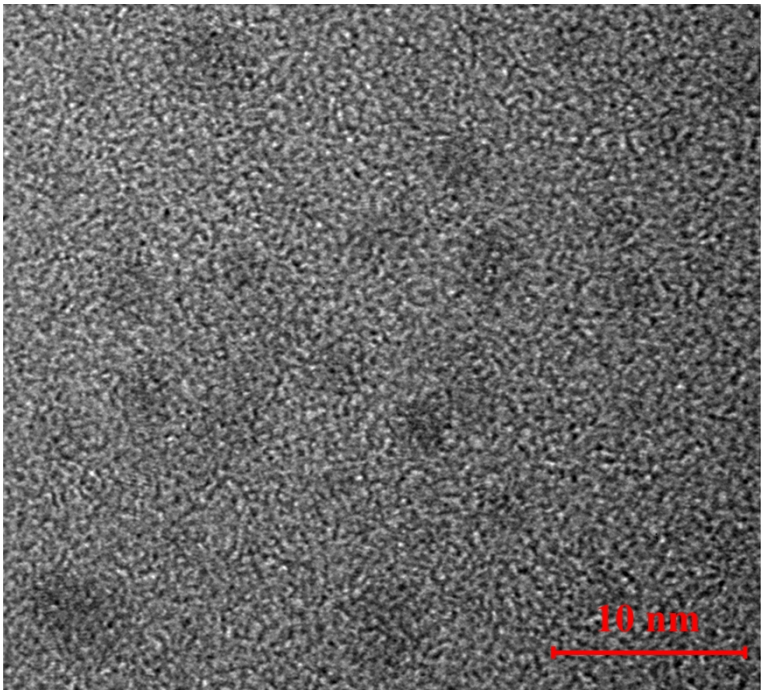

Fig. S4 HRTEM image of the as-prepared pure CDs (scale bar: 20 nm).

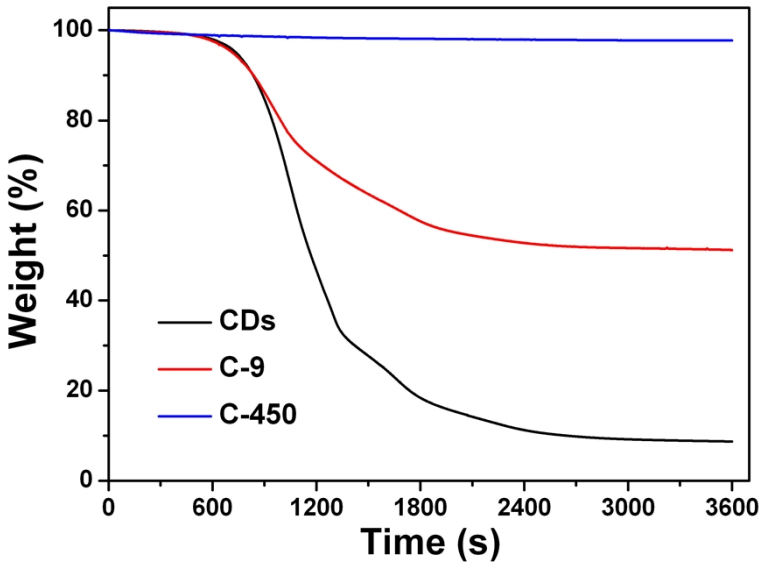

Fig. S5 Thermogravimetric curves of different samples from 50 ºC to 650 ºC under N_2 with a same heating rate (10 ºC per min).

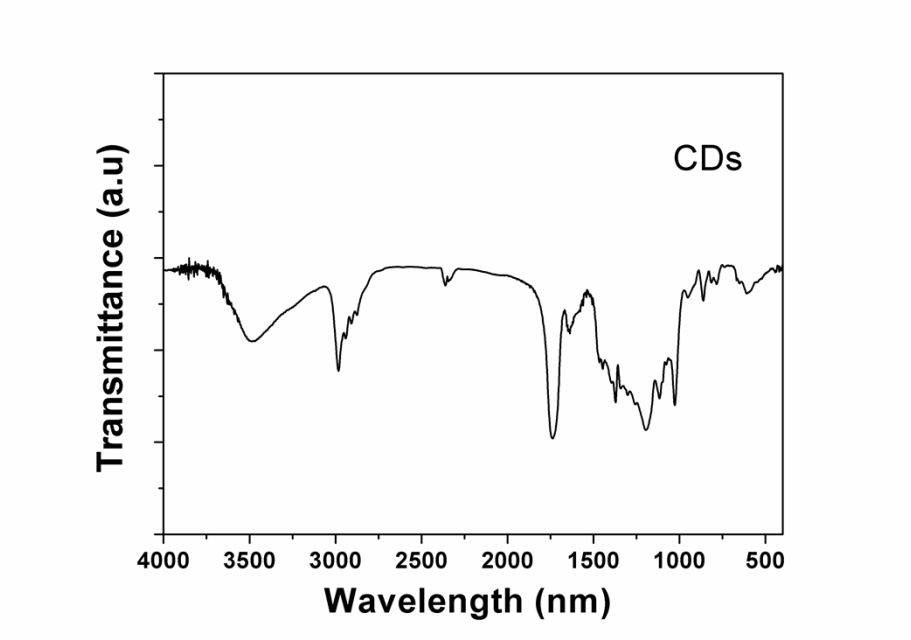

Fig. S6 FTIR spectrum of the as-prepared pure CDs.

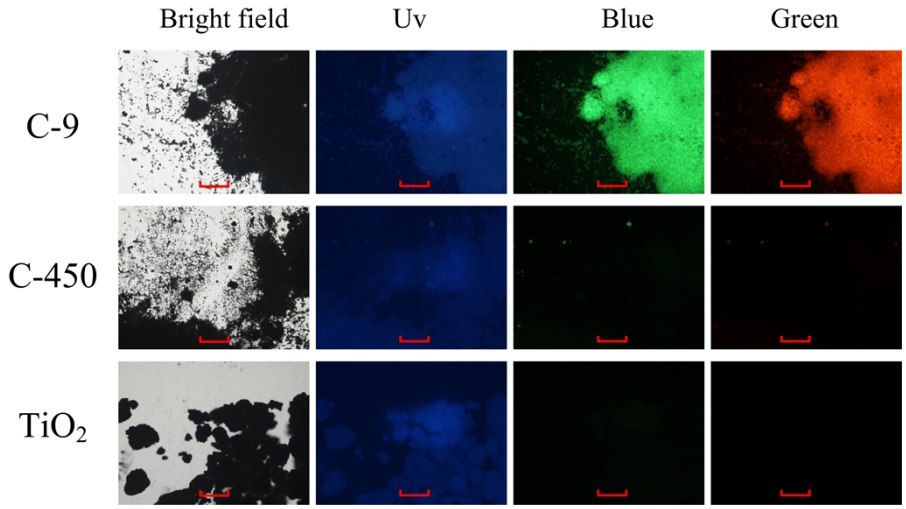

Fig. S7 Fluorescent microscopy images of C-9, C-450 and pure TiO_2 under the same photograph conditions.

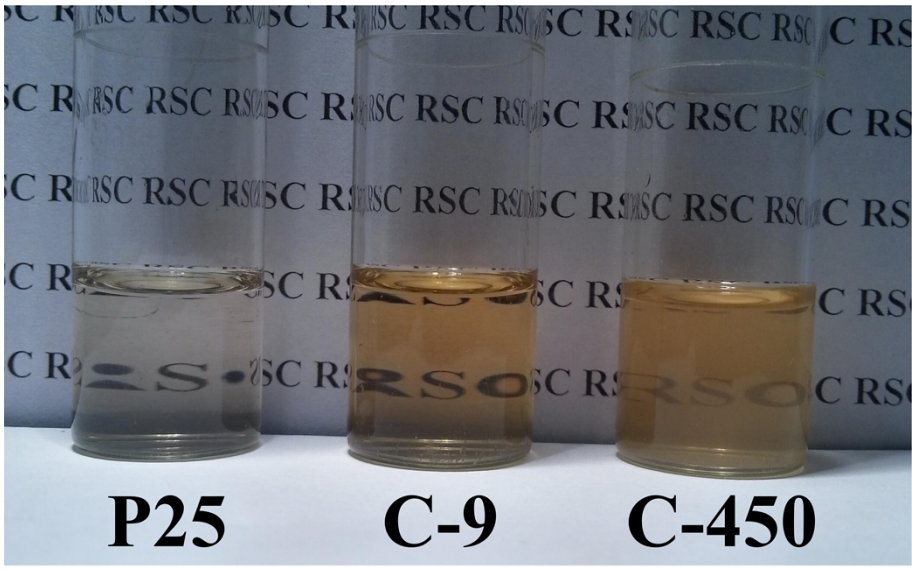

Fig. S8 Photographs of P25, C-9 and C-450 that dissolved in concentrated sulfuric acid under natural light.

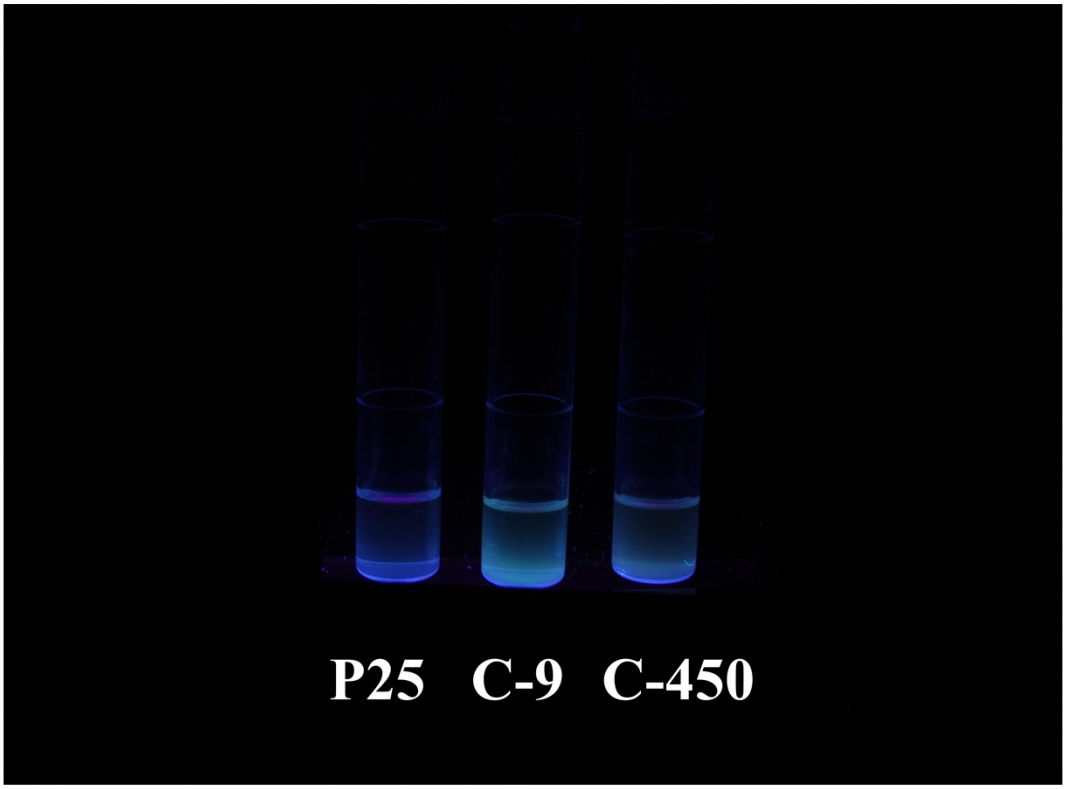

Fig. S9 Photographs of P25, C-9 and C-450 that dissolved in concentrated sulfuric acid under a UV lamp (365 nm).

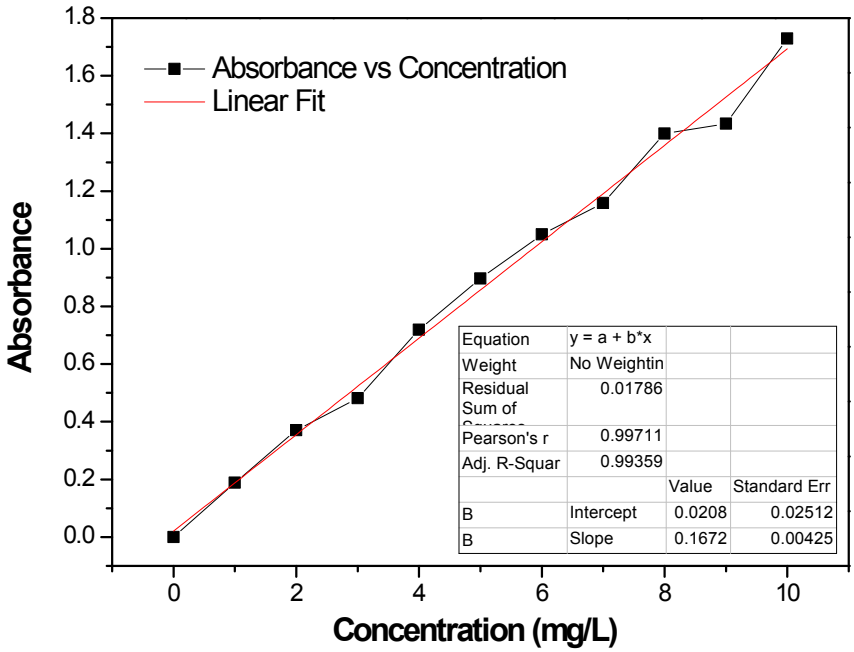

Fig. S10 UV-vis absorbency of the MB solution at 664 nm with different concentrations.

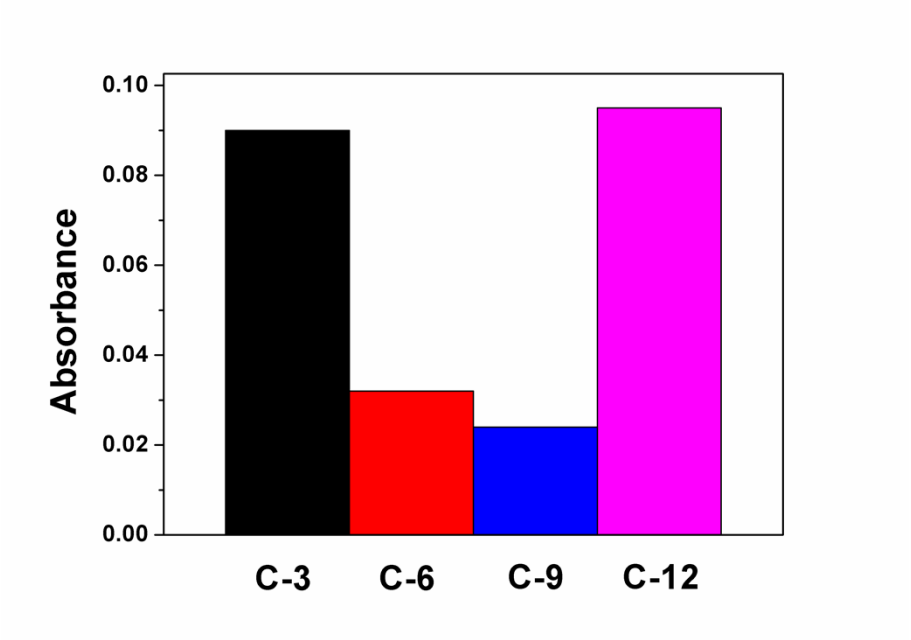

Fig. S11 UV-vis absorbance at 664 nm monitoring the photo-degradation efficiency of CDs-TiO_2 composites on MB after 10 min irradiation under UV light (254 nm).

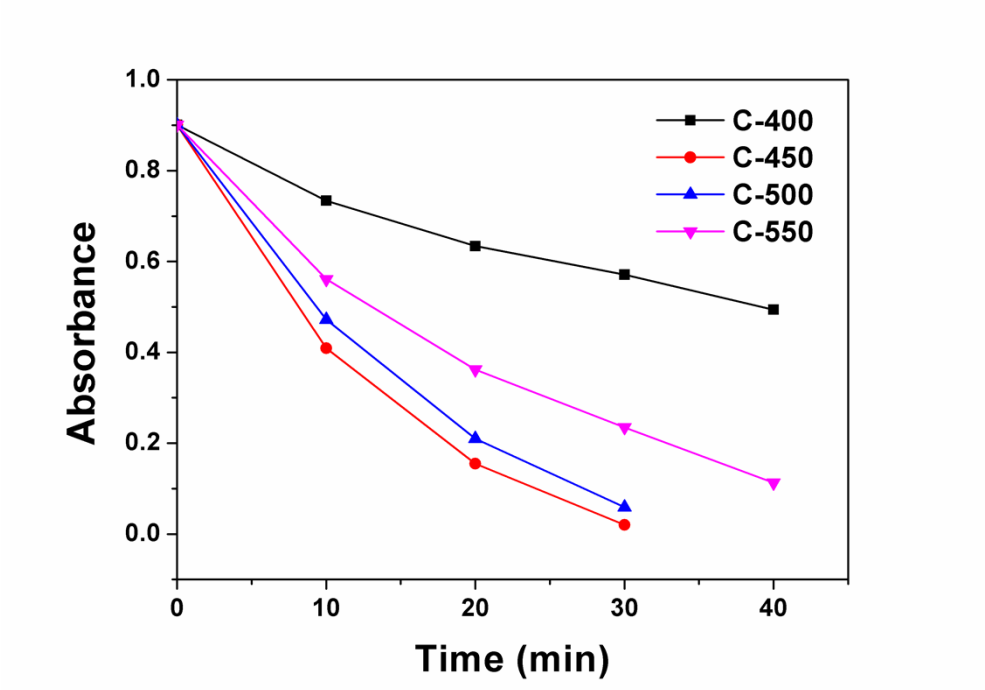

Fig. S12 UV-vis absorbance at 664 nm monitoring the photo-degradation efficiency of C-TiO_2 composites on MB at regular intervals under UV light (254 nm).

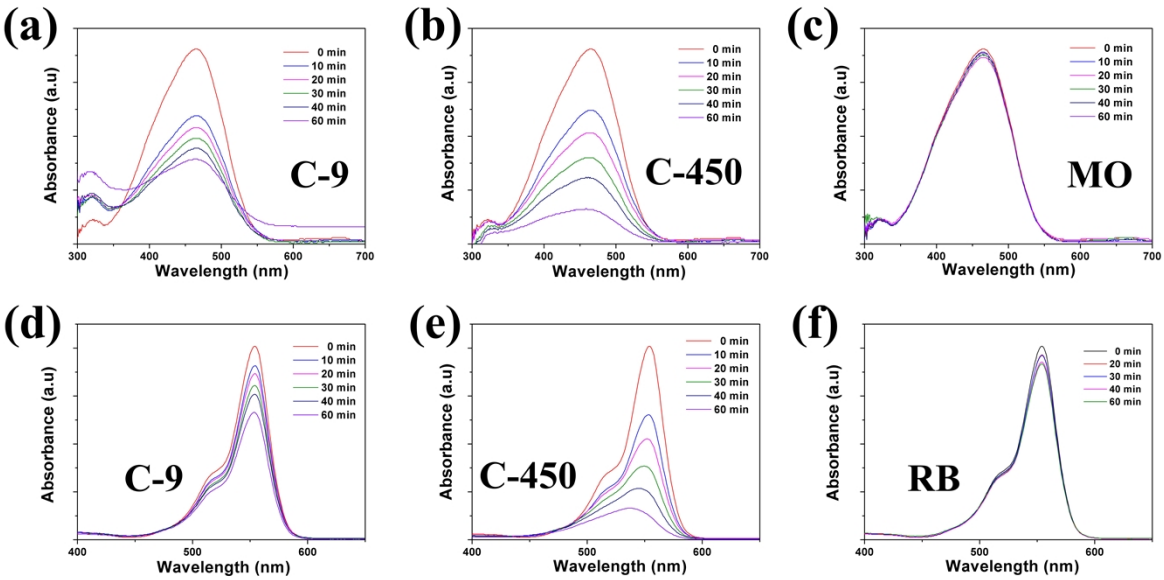

Fig. S13 UV-vis absorption spectra monitoring the degradation of MO (a, b and c) and RB (d, e and f): with C-9 as catalysts (a and d), with C-450 as catalysts (b and e) and without catalysts (c and f).

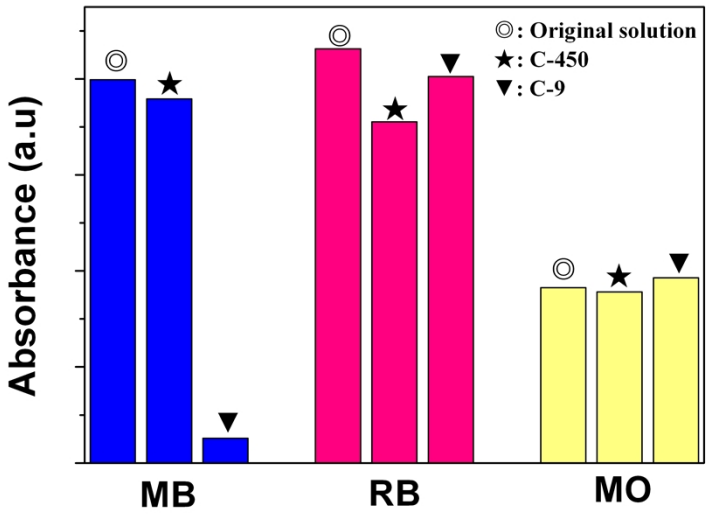

Fig. S14 Absorbance at 664 nm (MB), 554 nm (RB) and 462nm (MO) monitoring the absorption capacity of C-9 and C-450 upon the pollutants.

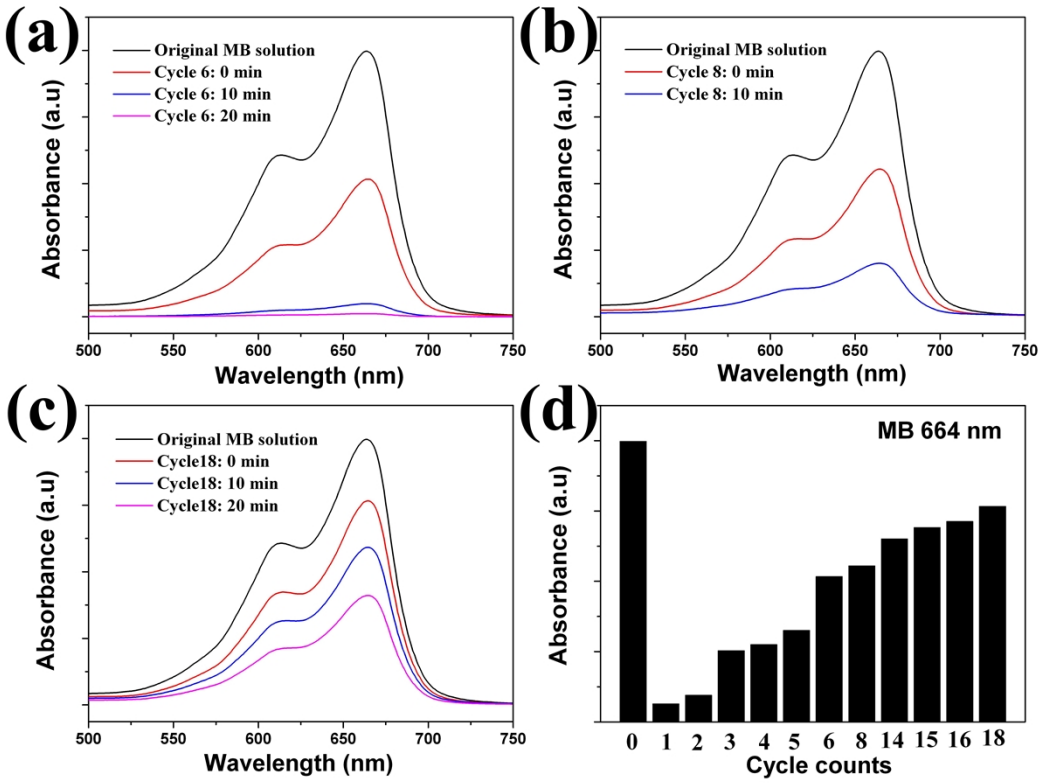

Fig. S15 UV-vis absorption spectra monitoring the degradation of MB (10 ppm) at different cycles using C-9 as the catalysts (a, b and c) and the absorbance at 664 nm monitoring the concentration of MB at the adsorption-desorption equilibrium of each cycle.